Deficiency of the base excision repair enzyme NEIL3 is associated with increased lymphocyte apoptosis, autoantibodies and predisposition to autoimmunity

Michel J. Massaad, Jia Zhou, Daisuke Tsuchimoto, Janet Chou, Haifa Jabara, Erin Janssen, Salomé Glauzy, Brennan Olson, Henner Morbach, Toshiro K. Ohsumi, Klaus Schmitz, Markianos Kyriacos, Jennifer Kane, Kumiko Torisu, Yusaku Nakabeppu, Luigi D. Notarangelo, Eliane Chouery, Andre Megarbane, Peter B. Kang, Eman Al-Idrissi, Hasan Aldhekri, Eric Meffre, Masayuki Mizui, George C. Tsokos, John P. Manis, Waleed Al-Herz, Susan S. Wallace, and Raif S. Geha.

Supplemental Materials

Supplemental Tables 1-4:

Supplemental Table 1. Frequency of mutations at A, C, G, and T in the J558V_HFR3-J_H4 and 3' intron segments of the *Igh* locus in pooled sequences from Peyer's patches germinal center B cells of the indicated genotypes.

Supplemental Table 2. Spectra of mutation in the J558V_HFR3-J_H4 and 3' intron segments in pooled sequences from Peyer's patches germinal center B cells of the indicated genotypes.

Supplemental Table 3. Primers used to amplify and mutagenize full length human *NEIL3*.

Supplemental table 4. Primers used for RT-PCR amplification of the indicated exons in the *LRBA* cDNA.

Supplemental Figures 1-4

Figure S1. Duplication of exons 49 to 53 of LRBA in Patient 3.

Figure S2. Normal lymphoid cell number and distribution in *Neil3*^{-/-} mice.

Figure S3. Normal T and B cell function in *Neil3*^{-/-} mice.

Figure S4. Normal serum immunoglobulins, red blood cell and platelet numbers, absence of autoantibodies on the surface of red blood cells and platelets, and normal architechture of kidneys isolated from *Neil3*^{-/-} mice.

SUPPLEMENTAL FIGURE LEGEND

Figure S1. Duplication of exons 49 to 53 of LRBA in Patient 3. (A) Single step RT-PCR analysis of LRBA cDNA from EBV-transformed B cells from Patient (Pt) 3 and a control (Ctrl), using primers specific to exons 48 through 54. A single product of the expected size is observed in Pt.3 using primers specific to exons 48 and 54. A normal and a larger band are observed in Pt.3 using primers specific to exons 49 through 53. The exon number and the expected size of the PCR amplicons are shown above the corresponding lanes in the gel. Data are representative of three independent experiments. **(B)** Schematic representation of the results obtained from the Sanger sequencing of the additional large PCR amplification products obtained from Pt.3 using primers specific to exons 49 through 53 of LRBA. The expected sizes of the normal and abnormal PCR amplicons are shown.

Figure S2. Normal lymphoid cell number and distribution in *Neil3$^{-/-}$* mice. (A) Thymus cellularity, representative FACS analysis of CD4$^+$ and CD8$^+$ cells, and percentages of CD4$^+$ and CD8$^+$ cells in the thymi of *Neil3$^{-/-}$* mice and *wild type* (WT) controls. **(B)** Bone marrow cellularity, representative FACS analysis of B220$^+$CD43$^+$ and B220$^+$IgM$^+$ cells, and percentages of pro-B, pre-B, immature, and mature B cells in the bone marrow of *Neil3$^{-/-}$* mice and WT controls. **(C-D)** Representative FACS analysis of B220$^+$, CD3$^+$, CD4$^+$, and CD8$^+$ cells in spleens (C) and inguinal lymph nodes (D) of *Neil3$^{-/-}$* mice and WT controls. Shown are the percentages of CD4$^+$ and CD8$^+$ cells within the CD3$^+$ population. **(E)** Representative FACS analysis of CD25$^+$FOXP3$^+$ cells within the CD4$^+$ population in the spleens and inguinal lymph nodes of *Neil3$^{-/-}$* mice and WT controls. Columns and bars in A-E represent mean±SEM of five mice per group. *P* values were obtained by 2-tailed Student's *t* test. NS, not significant.

Figure S3. Normal T and B cell function in *Neil3$^{-/-}$* mice. (A-B) In vitro proliferation (A) of, and cytokine secretion (B) by splenic T cells stimulated with immobilized anti-CD3 mAb alone, or in combination with soluble anti-CD28 or IL-2. **(C)** In vitro proliferation of unstimulated (unst.) WT Teff cells (shaded grey), or Teff cells stimulated (stimul.) with antigen presenting cells and anti-CD3 in the absence (blue) or presence (red) of Treg cells at a ratio of 1:1 Teff:Treg. Proliferation was assessed by FACS analysis of Cell Trace Violet dye dilution. The plot shows the percentage suppression of WT Teff cell proliferation using different ratios of WT or *Neil3$^{-/-}$* Treg cells. **(D-E)** In vitro proliferation (D), and IgE and IgG1 secretion (E) by purified splenic B cells stimulated with anti-CD40, IL-4, or LPS alone, or in combination. **(F-I)** In vivo IgM (F and H) and IgG (G and I) antibody responses of 8-12 week-old *Neil3$^{-/-}$* and WT mice immunized with the T-dependent antigen TNP-KLH (F-G), or the T-independent antigen TNP-Ficoll (H-I). TNP$_{32}$-BSA and TNP$_2$-BSA we used to determine low affinity and high affinity IgG production, respectively. Columns or squares and bars represent mean±SEM of five mice per group. *P* values were obtained by 2-tailed Student's *t* test (A-E) or 2-way ANOVA (F-I). NS, not significant. n.d., not detected.

Figure S4. Normal serum immunoglobulins, red blood cell and platelet numbers, absence of autoantibodies on the surface of red blood cells and platelets, and normal architechture of kidneys isolated from *Neil3$^{-/-}$* mice. (A-B) Serum immunoglobulin levels (A), and red blood cell and platelet numbers (B) in *Neil3$^{-/-}$* mice and wild type (WT) controls. *P* values were obtained by 2-tailed Student's *t* test. **(C)** FACS analysis of IgG bound to the surface of red blood cells (left panels), and platelets (right panels) isolated from 27 week old *Neil3$^{-/-}$* mice and WT controls. Cells were stained with FITC-labeled goat anti-mouse IgG, or goat anti-rabbit IgG as negative control. **(C)** Representative photomicrographs of periodic acid–schiff

(PAS)-stained kidney sections from 27-week old unmanipulated $Neil3^{-/-}$ mice and WT controls. The sections demonstrate normal glomeruli (white arrows), and absence of periglomerular and interstitial infiltrates in $Neil3^{-/-}$ mice and WT controls. The photomicrographs were taken at 20x magnification. Scale bars are shown. Ten mice in each group were used for A-D.

Supplemental Table 1. Frequency of mutations at A, C, G, and T in the J558V$_H$FR3-J$_H$4 and 3' intron segments of the *Igh* locus in pooled sequences from Peyer's patches germinal center B cells of the indicated genotypes.

	A	C	G	T	Total
WT	35.53 ± 2.31	19.26 ± 3.36	21.73 ± 1.09	23.48 ± 2.35	100
***Neil3*$^{-/-}$**	30.65 ± 3.98	31.01 ± 2.56	19.70 ± 0.579	18.70 ± 2.15	100
p	0.35	0.05	0.17	0.21	

Germinal center B cells were FACS-sorted from the Peyer's patches of 3 WT and 3 *Neil3*$^{-/-}$ mice. The J558V$_H$FR3-J$_H$4 and 3' intron segments of the *IgH* locus were amplified, cloned in the TOPO-TA cloning vector, and 200 clones from each mouse were Sanger-sequenced. A 551 bp fragment from each clone that excluded the V regions was analyzed for the presence of mutations, and compared to the reference sequence of the C57BL/6J strain. The data are presented as percentage of mutations at A, C, G, and T out of the total mutations detected.

Supplemental Table 2. Spectra of mutation in the J558V$_H$FR3-J$_H$4 and 3' intron segments in pooled sequences from Peyer's patches germinal center B cells of the indicated genotypes.

WT To

From		A	C	G	T	Total
	A		7.2 ± 0.9	17.6 ± 1.2	10.1 ± 1.1	34.9
	C	3.4 ± 0.4		4.3 ± 0.8	15.4 ± 2.6	23.1
	G	10.2 ± 1.0	6.3 ± 1.1		4.0 ± 0.4	20.5
	T	6.1 ± 0.81	11.0 ± 1.1	4.5 ± 0.4		21.6

Neil3$^{-/-}$ To

From		A	C	G	T	Total
	A		7.6 ± 1.1	13.9 ± 2.4	8.4 ± 0.14	29.9
	C	5.8± 1.1		7.3 ± 0.6*	17.4 ± 0.9	30.5
	G	10.7 ± 2.4	7.8 ± 2.3		2.5 ± 1.0	21.0
	T	6.3 ± 1.3	9.7 ± 1.8	2.7 ± 0.6		18.7

Germinal center B cells were FACS-sorted from the Peyer's patches of 3 WT and 3 *Neil3$^{-/-}$* mice. The J558V$_H$FR3-J$_H$4 and 3' intron segments were amplified, cloned in the TOPO-TA cloning vector, and 200 clones from each mouse were Sanger-sequenced. A 551 bp fragment from each clone was analyzed for the presence of mutations, and compared to the reference sequence of the C57BL/6J strain. * p = 0.04

The data are presented as percentage of mutations, corrected for the base composition of the 551 bp segment. Base composition is as follows: A, 26.68%; C, 15.79%; G, 27.22%; T, 30.31%.

Supplemental Table 3. Primers used to amplify and mutagenize full length human *NEIL3* that was used for the immunoprecipitation-coupled glycosylase activity assays.

Primers	Sequences
NEIL3FL_For	5' CCGGGATCCATCATGGTGGAAGGTCCAGGCTGTACTC 3'
NEIL3FL_Rev	5' ATAAGAATGCGGCCGCTTTAAGCGTAGTCTGGGACGTCGTATG 3'
D132V_For	5' GATTTGATTTGTTTCTTTGTGTCATCAGTAGAACTCCG 3'
D132V_Rev	5' CGGAGTTCTACTGATGACACAAAGAAACAAATCAAATC 3'

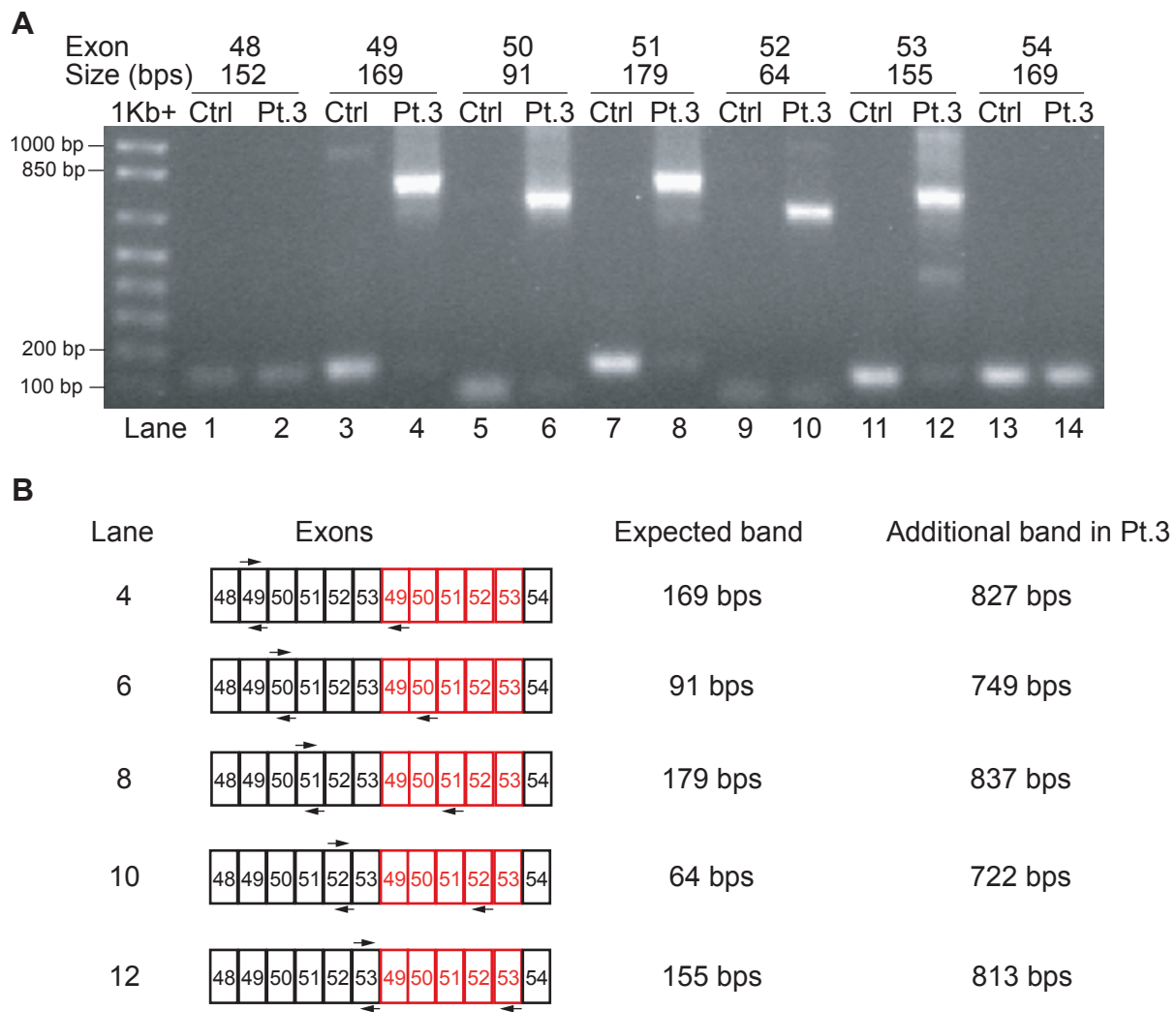NEIL3FL_For, sense primer used to PCR full-length the human *NEIL3* cDNA.

NEIL3FL_Rev, anti-sense primer used to PCR the full-length human *NEIL3* cDNA.

D132V_For, sense primer used to introduce the c.395_396AC>TG mutation in the full-length human *NEIL3* cDNA.

D132V_Rev, anti-sense primer used to introduce the c.395_396AC>TG mutation in the full length human *NEIL3* cDNA.

Supplemental table 4. Primers used for RT-PCR amplification of the indicated exons in the *LRBA* cDNA.

Exon	Sense primer	Antisense primer
Exon 1-28	5' TGCATTGCGTGTGTTGTGCTCA 3'	5' TATCCATGTCCTGTAGAAGCCT 3'
Exon 23-58	5' GATGTTTCCAATGTTGCTACAGA 3'	5' TGATGCTCCAGGTACTTCTGCT 3'
Exon 48	5' AGTTGATCCCTGAATTTTATTATCT 3'	5' CAATCTGTTTATGTGAACAAATTCT 3'
Exon 49	5' GCCCTGGAGAGTGAATTTGTT 3'	5' CTCTCTCAACACAGGATCAGT 3'
Exon 50	5' GCTGTTGAAGCTCAAATCCGA 3'	5' CACTTGCATGGCAGAACCTCT 3'
Exon 51	5' AGTCCATTGATGTTCACAGACA 3'	5' CAGGAAGGTTGTGCCATTTGT 3'
Exon 52	5' CTCATCAAGGTGCTGTACAAGA 3'	5' CTATGAGAGGATCGATTTCCA 3'
Exon 53	5' CCAGCAATACAGGAATGCACA 3'	5' CTGTGTCTGTAGAATAGACTCT 3'
Exon 54	5' GAAGATTGATCCAAGTGGTGT 3'	5' TGCCTGGGTTATCTCCAATCCCA 3'

Figure S1. Duplication of exons 49 to 53 of *LRBA* in Patient 3. (A) Single step RT-PCR analysis of *LRBA* cDNA from EBV-transformed B cells from Patient (Pt) 3 and a control (Ctrl), using primers specific to exons 48 through 54. A single product of the expected size is observed in Pt.3 using primers specific to exons 48 and 54. A normal and a larger band are observed in Pt.3 using primers specific to exons 49 through 53. The exon number and the expected size of the PCR amplicons are shown above the corresponding lanes in the gel. Data are representative of three independent experiments. **(B)** Schematic representation of the results obtained from the Sanger sequencing of the additional large PCR amplification products obtained from Pt.3 using primers specific to exons 49 through 53 of *LRBA*. The expected sizes of the normal and abnormal PCR amplicons are shown.
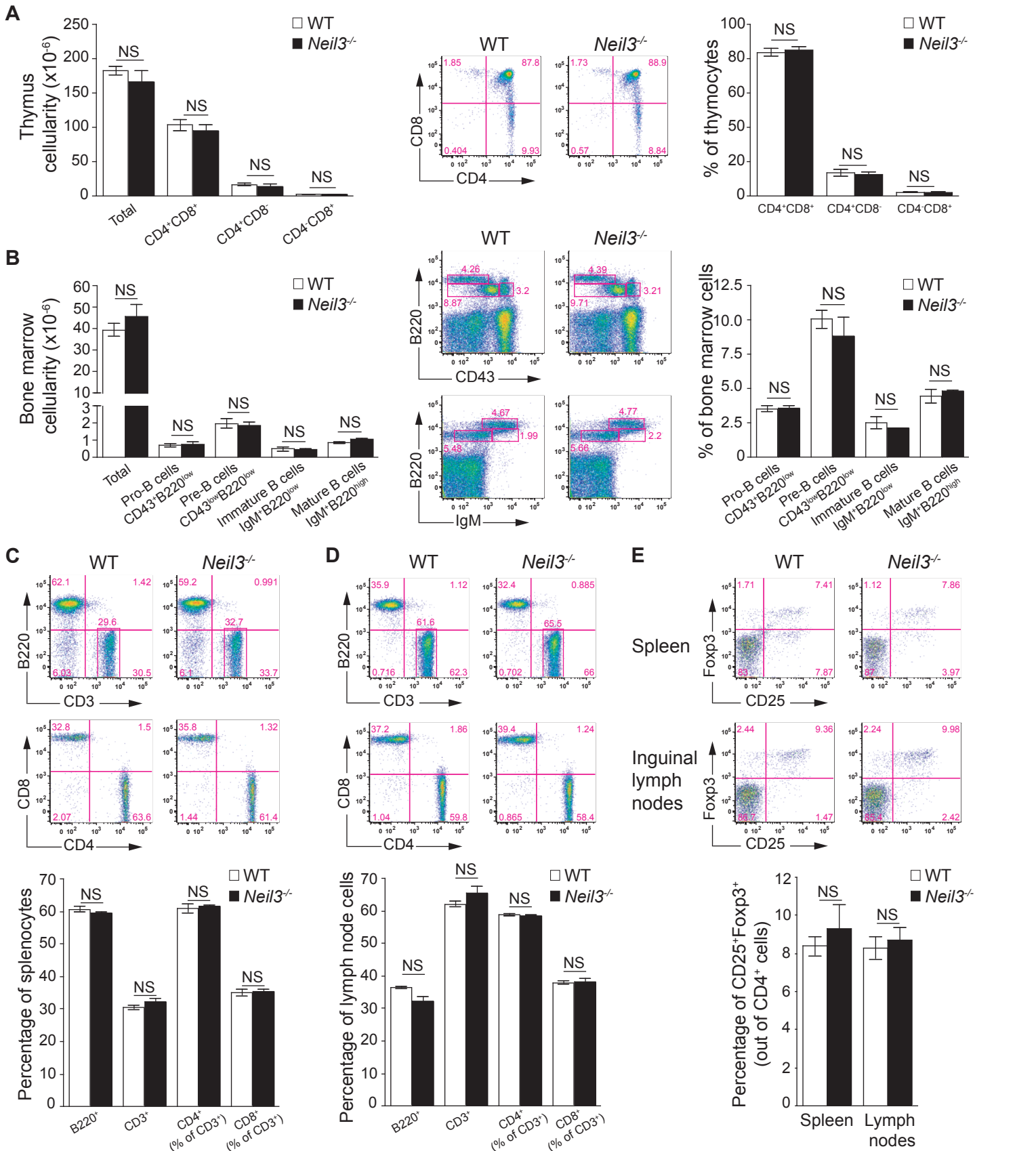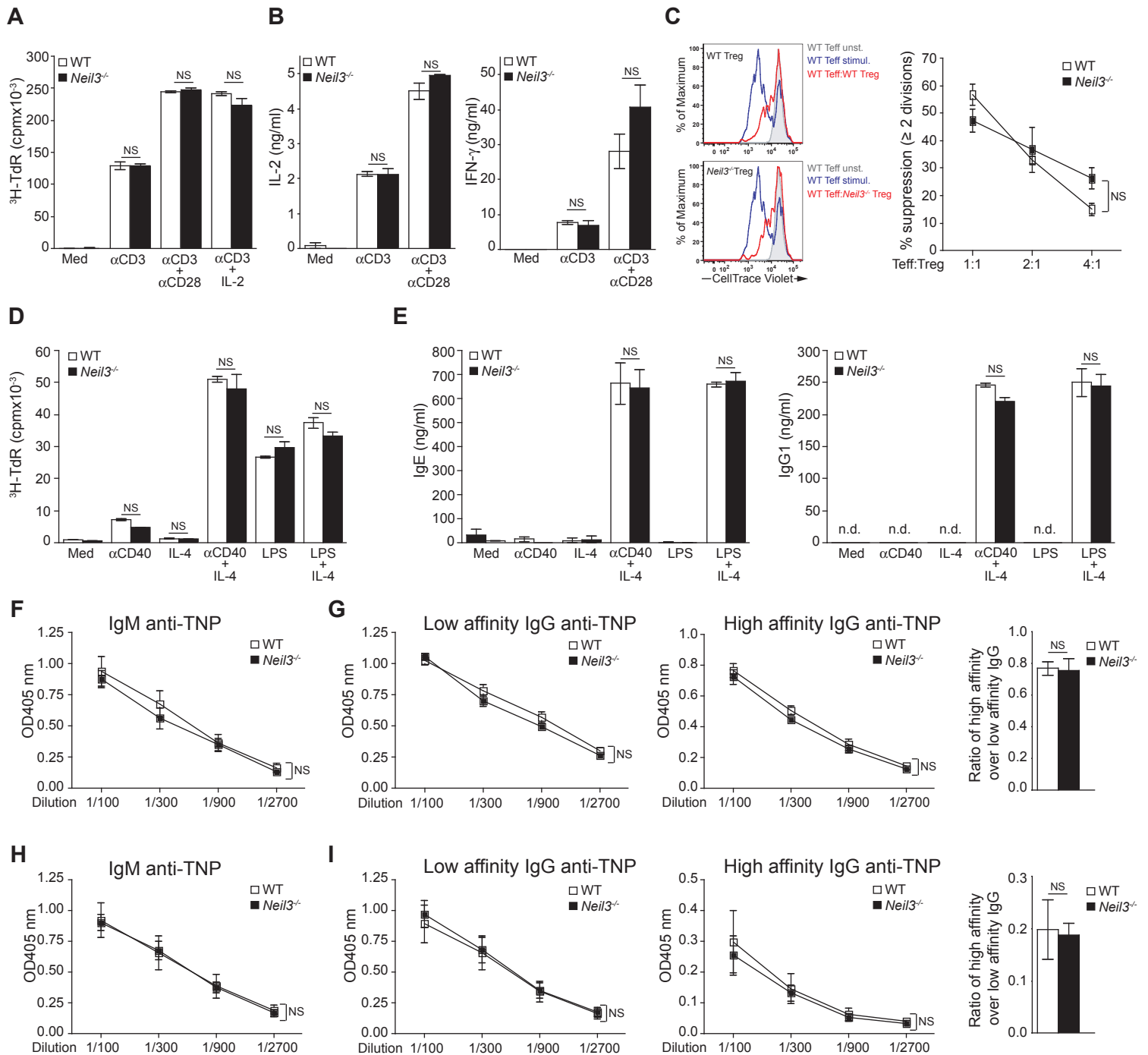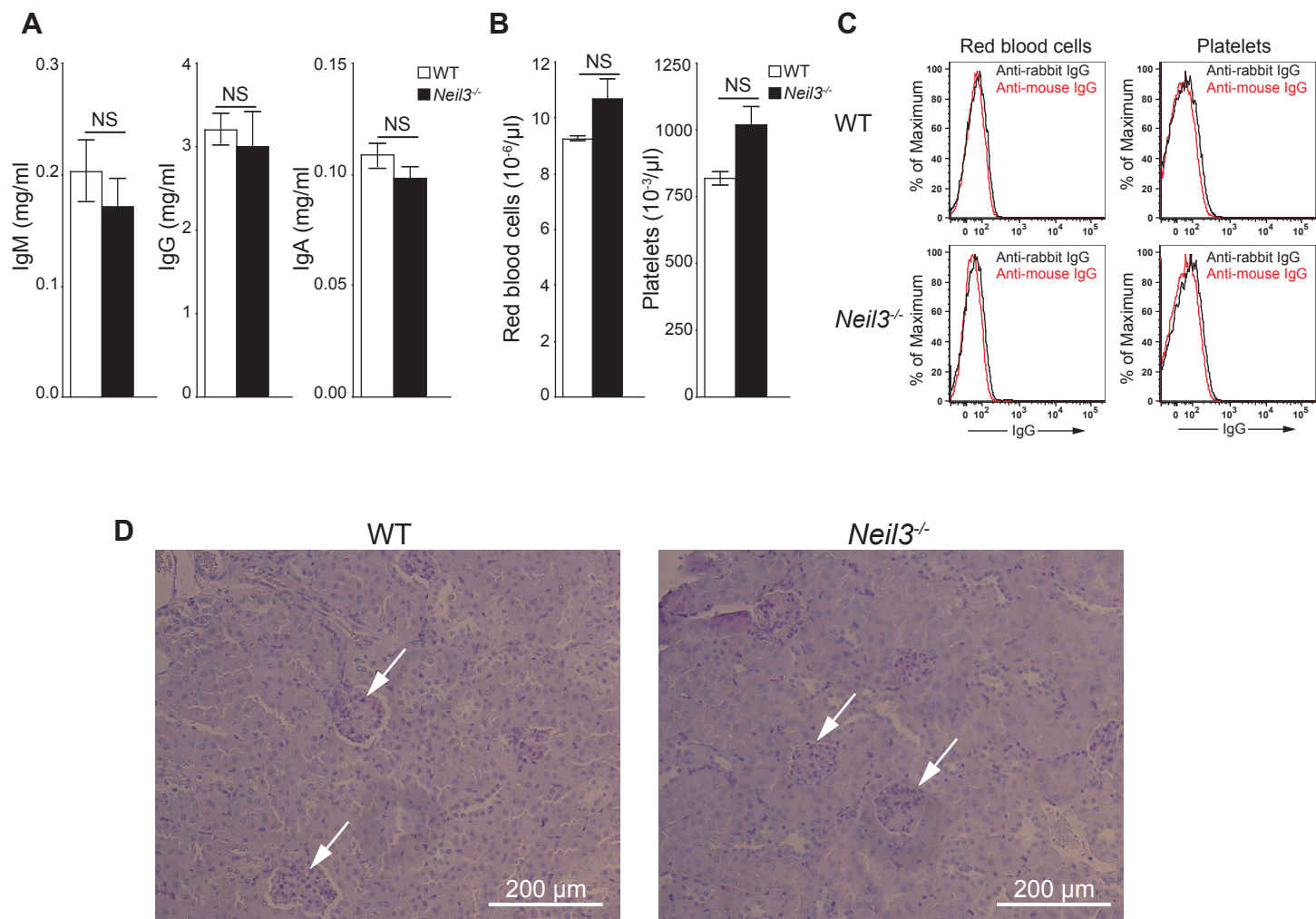
Figure S1

Figure S2. Normal lymphoid cell number and distribution in *Neil3*-/- mice. (A) Thymus cellularity, representative FACS analysis of CD4+ and CD8+ cells, and percentages of CD4+ and CD8+ cells in the thymi of *Neil3*-/- mice and *wild type* (WT) controls. **(B)** Bone marrow cellularity, representative FACS analysis of B220+CD43+ and B220+IgM+ cells, and percentages of pro-B, pre-B, immature, and mature B cells in the bone marrow of *Neil3*-/- mice and WT controls. **(C-D)** Representative FACS analysis of B220+, CD3+, CD4+, and CD8+ cells in spleens (C) and inguinal lymph nodes (D) of *Neil3*-/- mice and WT controls. Shown are the percentages of CD4+ and CD8+ cells within the CD3+ population. **(E)** Representative FACS analysis of CD25+FOXP3+ cells within the CD4+ population in the spleens and inguinal lymph nodes of *Neil3*-/- mice and WT controls. Columns and bars in A-E represent mean±SEM of five mice per group. *P* values were obtained by 2-tailed Student's *t* test. NS, not significant.

Figure S2

Figure S3. Normal T and B cell function in *Neil3⁻/⁻* mice. (A-B) In vitro proliferation (A) of, and cytokine secretion (B) by splenic T cells stimulated with immobilized anti-CD3 mAb alone, or in combination with soluble anti-CD28 or IL-2. **(C)** In vitro proliferation of unstimulated (unst.) WT Teff cells (shaded grey), or Teff cells stimulated (stimul.) with antigen presenting cells and anti-CD3 in the absence (blue) or presence (red) of Treg cells at a ratio of 1:1 Teff:Treg. Proliferation was assessed by FACS analysis of CellTrace Violet dye dilution. The plot shows the percentage suppression of WT Teff cell proliferation using different ratios of WT or *Neil3⁻/⁻* Treg cells. **(D-E)** In vitro proliferation (D), and IgE and IgG1 secretion (E) by purified splenic B cells stimulated with anti-CD40, IL-4, or LPS alone, or in combination. **(F-I)** In vivo IgM (F and H) and IgG (G and I) antibody responses of 8-12 week-old *Neil3⁻/⁻* and WT mice immunized with the T-dependent antigen TNP-KLH (F-G), or the T-independent antigen TNP-Ficoll (H-I). TNP$_{32}$-BSA and TNP$_2$-BSA were used to determine low affinity and high affinity IgG production, respectively. Columns or squares and bars represent mean±SEM of five mice per group. *P* values were obtained by 2-tailed Student's *t* test (A-E) or 2-way ANOVA (F-I). NS, not significant. n.d., not detected.

Figure S3

Figure S4. Normal serum immunoglobulins, red blood cell and platelet numbers, absence of autoantibodies on the surface of red blood cells and platelets, and normal architechture of kidneys isolated from *Neil3*⁻/⁻ mice. (A-B) Serum immunoglobulin levels (A), and red blood cell and platelet numbers (B) in *Neil3*⁻/⁻ mice and *wild type* (WT) controls. *P* values were obtained by 2-tailed Student's *t* test. **(C)** FACS analysis of IgG bound to the surface of red blood cells (left panels), and platelets (right panels) isolated from 27-week old *Neil3*⁻/⁻ mice and WT controls. Cells were stained with FITC-labeled goat anti-mouse IgG, or goat anti-rabbit IgG as negative control. **(C)** Representative photomicrographs of periodic acid–schiff (PAS)-stained kidney sections from 27 week old unmanipulated *Neil3*⁻/⁻ mice and WT controls. The sections demonstrate normal glomeruli (white arrows), and absence of periglomerular and interstitial infiltrates in *Neil3*⁻/⁻ mice and WT controls.
The photomicrographs were taken at 20x magnification. Scale bars are shown. Ten mice in each group were used for A-D.